JOURNAL OF SYNCHROTRON RADIATION

ISSN 1600-5775

Counting-loss correction for X-ray spectra using the pulse-repairing method

Lin Tang,[a,b] Jianbin Zhou,[b]* Fang Fang,[b] Jie Yu,[b] Xu Hong,[b] Xianli Liao,[a,b] Chuanwei Zhou[b] and Songke Yu[b]

[a]School of Information Science and Engineering, Chengdu University, No.1 Shiling Street, Longquanyi District, Chengdu 610106, People's Republic of China, and [b]College of Nuclear Technology and Automation Engineering, Chengdu University of Technology, No. 1 East 3 Road, ErXianbrige, Chenghua District, Chengdu 610059, People's Republic of China. *Correspondence e-mail: zjb@cdut.edu.cn

Received 6 August 2018
Accepted 5 October 2018

Edited by S. Svensson, Uppsala University, Sweden

Keywords: counting-loss correction; fast SDD; pulse repairing; peak area; X-ray spectrum.

Facing the technical problem of pulse distortion caused by frequent resetting in the latest high-performance silicon drift detectors, which work under high-counting-rate conditions, a method has been used to remove false peaks in order to obtain a precise X-ray spectrum, the essence of which eliminates distorted pulses. Aiming at solving the problem of counting-loss generated by eliminating distorted pulses, this paper proposes an improved method of pulse repairing. A ^{238}Pu source with activity of 10 mCi was used as the measurement object, and the energy spectrum obtained by the pulse repairing method was compared with that obtained by the pulse elimination method. The ten-measurement results show that the pulse repairing method can correct the counting-loss caused by the pulse elimination method and increase peak area, which is of great significance for obtaining a precise X-ray energy spectrum.

1. Introduction

In recent years, energy-dispersive X-ray fluorescence technology has been developing toward high counting rate and high energy resolution. To obtain a pulse signal with high signal-to-noise ratio (SNR) and low trajectory loss in the context of high counting rate, most semiconductor detectors have integrated the switch reset preamplifier internally (Jakobson & Nemirovsky, 1995, 1997; Sun *et al.*, 2005). The output signal of the preamplifier is a series of pile-up pulses with fast exponential rising edge. When the pulses accumulate to a certain level, the last pulse will jump to zero and then the next round of pile-up starts. If we directly filter and shape the rising stacking pulses, counting-rate losses will occur due to pulse amplitude overflow. In order to obtain a precise spectrum with good energy resolution and high counting rate, we need to amplify and digitize the output nuclear signal and then filter and shape it properly (Morse, 2010). In previous research we have proposed a method to remove false peaks by eliminating distorted pulses (Tang *et al.*, 2018). After further research, we find that the method of eliminating distorted pulses can be used to eliminate false peaks, but there is a counting-rate loss defect.

In view of the above defect, this paper, which is based on the previous research results described by Tang *et al.* (2018), proposes a new method of pulse repairing to repair the distorted negative exponential signal. The trapezoidal/triangular shaping result of the repaired negative exponential signal is in good agreement with the shaping result of a complete negative exponential signal. Finally, this method guarantees the counting rate successfully and increases peak

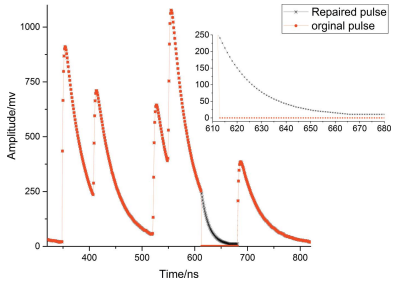

area. The feasibility and accuracy of the method is verified by simulation and experiment. The results show that this method can effectively improve the counting rate and the peak area, and enhance the detection accuracy of weak elements in complex samples.

2. Circuit description

In nuclear electronics, preamplifiers are usually divided into three types, *i.e.* the current-sensitive, charge-sensitive and voltage-sensitive preamplifier. For mathematical models of the output signal, however, the preamplifier is further divided into a resistance capacitance coupled preamplifier and a switch reset preamplifier (Sun *et al.*, 2005). The switch reset preamplifier is widely used in semiconductor detectors because of its advantages of high signal-to-noise ration (SNR) and small ballistic loss; a circuit diagram of a switch reset preamplifier is shown in Fig. 1. The amplifier usually adopts a FET transconductance operational amplifier with low noise, but whose bandwidth and input capacitance are usually large, which is not conducive to obtaining a high SNR. Therefore, the choice of parameters for the feedback resistance usually requires a compromise.

The switch reset preamplifier circuit comprises an operational amplifier, an integral capacitor and an analog switch, whose principle is that the output current of the semiconductor detector is integrated in the feedback capacitance C_f, for an integral time t, and the integral results are stored in the holding capacitor C_f to be measured by the follow-up measurement circuit. Finally, we will obtain a voltage, which is proportional to the current and integral time. The length of the integral period is controlled by an artificially set time sequence, which is set according to the request of the input current and the signal acquisition speed. Because the integral effect is equivalent to low-pass filtering, the switch reset preamplifier circuit has a good restraining effect on high-frequency noise, especially for periodic interference and noise, such as AC 50 Hz. Therefore, an amplifying circuit that adopts this kind of design can maintain a good noise performance without additional filtering networks (Zhen *et al.*, 2002).

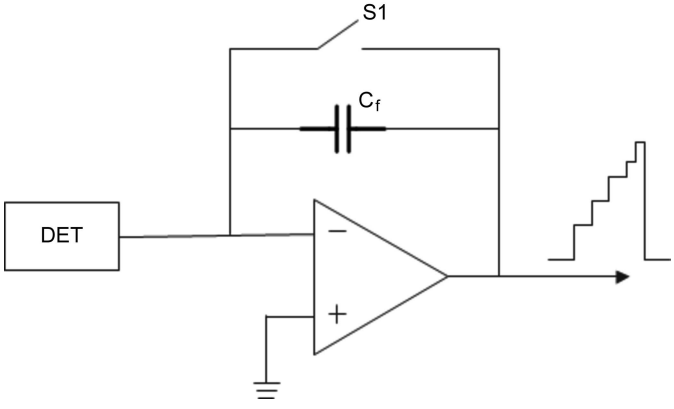

Figure 1
Switch reset preamplifier circuit.

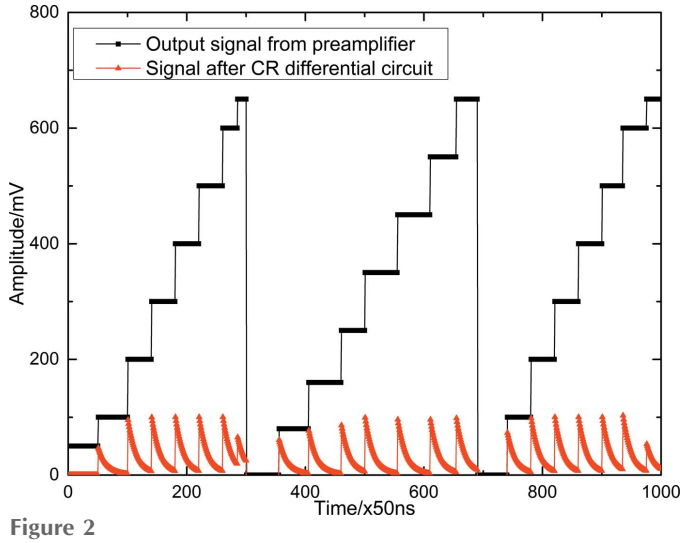

Figure 2
Output signal of the step signal after the CR differential circuit.

As shown in Fig. 2, the output signal of the switch reset preamplifier is a series of rising pile-up pulses. When the step pulses are piled up to a certain extent, the feedback capacitance charging is completed, and then switch S1 will control the feedback capacitance to discharge and reset. At the same time, the output pulse of the preamplifier jumps from the peak value to zero, and then a new round of pulse pile-up begins. Considering that the output signal of the preamplifier is rising and jumping frequently, if we directly amplify the signal and digitalize it, the result will cause impulse overflow and counting-rate loss. Therefore, before nuclear signals experience the shaping process in a field programmable gate array (FPGA), step signals need to be transmitted into negative exponential signals by a capacitance resistance (CR) differential circuit, which can not only complete the signal conversion but also filter high-frequency noise (Wang *et al.*, 2018). The step signals and the negative exponential signals transmitted by the CR differential circuit are shown in Fig. 2. As shown in this figure, the jumping time of each pulse is uncertain, so the last step pulse is likely to be a distorted pulse, whose holding time is insufficient; then, this distorted pulse passes through the CR differential circuit and a distorted negative exponential pulse will be generated. If we directly eliminate the distorted negative exponential pulses without repairing them, false peaks caused by the distorted pulse will appear in front of the full energy peak in the final spectrum, and at the same time the count rate would be reduced.

3. Pulse repairing method

In the previous research results (Tang *et al.*, 2018), high-resolution real-time pulse shaping adopts a trapezoidal/triangular shaping method. For the distorted negative exponential pulses, because the shaping results are affected by the moment of reset, based on the time of pulse distortion, the pulse shape discrimination unit will distinguish whether the distorted pulses should be eliminated or not. When the pulse counting rate is high, the reset frequency is also high, and then the

number of distorted pulses will also increase. If the quantity of distorted pulses discarded increases, the whole counting rate will decrease. Therefore, based on the method which eliminates all distorted pulses, a new method for repairing distorted pulses is proposed to ensure the counting rate while eliminating false peaks.

In the classic spectroscopy system, a preamplifier integrated in the detector will usually follow a high-pass filter (pole-zero cancellation, CR differential circuit), which will generate a negative exponential pulse with short rise time and exponential tailing (Jordanov *et al.*, 1994*a*). After the next stage of magnification, a high-precision analog-to-digital converter (ADC) digitalizes the negative exponential pulse and then both the location and repairing process of the distorted pulses will be completed in the FPGA.

Theoretically, when we need to repair the pulses with exponential features, the best method is to calculate the value of the next sampling point by using an exponential function expression. The decay trend of the pulse repaired by this method is only controlled by the time constant τ, so the repairing result is basically the same as the original pulse. However, it is difficult to realize the iteration and calculation in the exponential form in the FPGA, especially when τ is unknown. Therefore, this paper also proposes a multi-order successive approximation method to repair the distorted pulse, which can adjust the velocity of decay by the order of the successive approximation method. The two repairing methods will be introduced in detail in the following.

3.1. τ restoration method

The expression for the negative exponential signal is shown in equation (1) (Zhou *et al.*, 2017),

$$\begin{aligned} v(n) &= A\exp\left(-n\,T_{\rm CLK}/\tau\right) \\ &= A\exp\left[-(n-1)\,T_{\rm CLK}/\tau\right]\exp\left(-T_{\rm CLK}/\tau\right). \end{aligned} \tag{1}$$

Here, $v(n)$ always equals zero for $n < 0$, $T_{\rm CLK}$ is the sample frequency and τ is the decay time constant. In view of the limited space here, the focus of this paper is repairing of the distorted pulse and comparison of the actual measurement results after the repairing. Jordanov *et al.* (1994*b*) and Jordanov (1994) describe the recursive algorithm derivation of the trapezoid/triangular shaper in detail, which realizes the transformation from a digital negative exponential pulse to a symmetric trapezoidal pulse by delay line, adder/subtractor and accumulator.

In the derivation of the trapezoid/triangular shaping algorithm, $d^{k,l}(n)$ can be expressed as a consequence of two identical procedures given by the set of equations

$$d^{k}(n) = v(n) - v(n-k), \tag{2}$$

$$d^{k,l}(n) = d^{k}(n) - d^{k}(n-l). \tag{3}$$

The unit that implements the algorithm of equation (2) or equation (3) contains two functional elements: a programmable delay pipeline and a subtractor.

A digital pole-zero cancellation circuit is realized by equations (4) and (5), whose output response is $r(n)$. The last block of the trapezoidal/triangular shaper is an accumulator which implements the algorithm given by equation (6),

$$p(n) = p(n-1) + d^{k,l}(n), \tag{4}$$

$$r(n) = p(n) + M\,d^{k,l}(n), \tag{5}$$

$$s(n) = s(n-1) + r(n). \tag{6}$$

The parameter M depends only on the decay time constant τ and the exponential pulse and the sampling period $T_{\rm CLK}$ of the digitizer, and is given by

$$M = \frac{1}{\exp\left(T_{\rm CLK}/\tau\right) - 1}. \tag{7}$$

We can conclude equation (8) in the basis of equation (7),

$$\exp\left(-\frac{T_{\rm CLK}}{\tau}\right) = \frac{M}{1+M}. \tag{8}$$

Then, we obtain the theoretical basis of the pulse repairing, which is given by

$$v(n) = A\exp\left[-(n-1)\,T_{\rm CLK}/\tau\right]\frac{M}{1+M}. \tag{9}$$

For values of $T_{\rm CLK}/\tau > 5$, the Taylor expansion of equation (7) can be approximated as

$$M \simeq \frac{\tau}{T_{\rm CLK}} - 0.5. \tag{10}$$

Take any one digitalized distorted negative index signal, as shown in Fig. 3. By reading the coordinates of the known sampling points we can calculate the time constant τ, the amplitude A and the sampling period $T_{\rm CLK}$. Here, $\tau = 100$, $A = 2000$, $T_{\rm CLK} = 1$, and $M \simeq \tau = 100$ is known on the basis of equation (10). In this paper, a complete negative exponential signal is made up of 1024 sampling points, but the distorted negative exponential pulses directly jump to zero from the

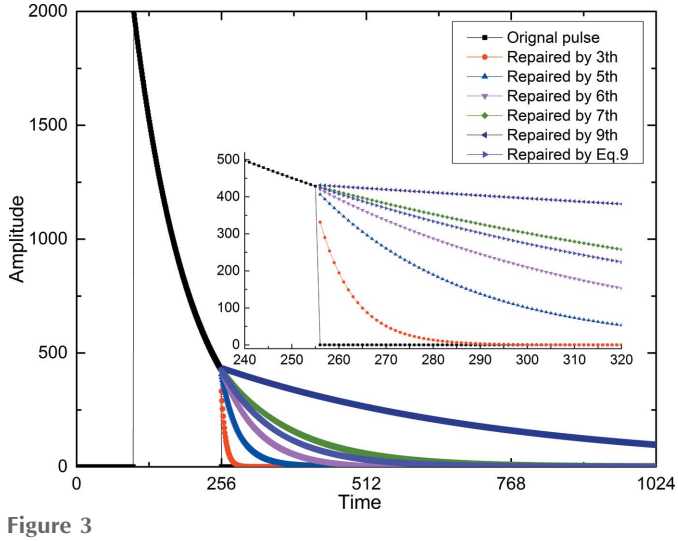

Figure 3
Contrast figure of pulse repairing.

250th sample point during the decay process; that is to say, all the impulse information after the 250th sampling points is lost. In order to repair the distorted pulses, we employ MATLAB software and regard equation (9) as a theoretical basis for repairing. Knowing $M \simeq \tau = 100$, $A = 2000$, $T_{\rm CLK} = 1$, and substituting these parameters into equation (9) we obtain 774 sampling points, which are all lost sample points caused by pulse distortion. The repairing result is shown in Fig. 3, which is consistent with the decay trend of the original pulse.

3.2. Multi-order successive approximation method

The key to the successive approximation method is to select optimal orders (the essence of this method is to find the ideal decay speed at which the repaired curve can match the decay trend of the original curve at the maximum extent). This method was realized by means of addition and division, whose implementation process is depicted as follows.

A result is repaired by the first-order successive approximation method,

$$v_1(n+1) = \big[v(n) + 0\big]/2. \tag{11}$$

A result is repaired by the second-order successive approximation method,

$$v_2(n+1) = \big[v(n) + v_1(n+1)\big]/2. \tag{12}$$

A result is repaired by the mth-order successive approximation method,

$$v_m(n+1) = \big[v(n) + v_{m-1}(n+1)\big]/2. \tag{13}$$

This paper assumes that the negative exponential signal $v(n)$ has lost all the sampling points after n. In view of the limited space here, we only list part of the successive approximation method; the rest is derived by iterative method, as shown in equation (13).

Based on equations (11)–(13), we can calculate all lost sampling points and draw the contrast figure of pulse repairing, which is repaired by different methods, as shown in Fig. 3. From this figure we can conclude that the higher the order of the successive approximation method, the slower the decay of the curve. The repairing results of the third-order and the fifth-order successive approximation methods have a fast decay velocity, which does not match the decay trend of the original curve. The seventh-order successive approximation method has a good repairing result, but the decay speed is slow when the ninth-order successive approximation method is used. The repairing result of equation (9), which is derived from the exponential recursive algorithm, is slightly better than the repairing result of the seventh-order successive approximation method. In the comparison of the repair effects that will be discussed in the *Experiment tests* section (§4), the X-ray spectrum obtained by the repair of equation (9) and the seven-order successive approximation method are compared; the differences between the two repair methods are quantified on the basis of the comparison results.

3.3. Method verification

In the last part, we put forward a recursive algorithm and the seventh-order successive approximation method to repair the distorted negative exponential pulse. We finally decided to employ the seventh-order successive approximation method as the pulse repairing method in this paper. Here, we depict the comparison of shaping results of a complete negative exponential signal and a repaired negative exponential signal by the seventh-order successive approximation method, shown in Fig. 4. If the comparison results are indeed consistent, the feasibility of the seventh-order successive approximation method mentioned above can be verified.

In the spectral measurement process, the FPGA is the key to the whole digital nuclear signal processing, which mainly realizes two processes of pulse repairing and pulse shaping. Due to limited space in this paper, here we mainly focus on the study of pulse repairing and verifying the repairing method through a simulation result of trapezoidal/triangular shaping (Jordanov, 2003; Menaa *et al.*, 2011). Considering that pulse shaping has been introduced in our previous research (Tang *et al.*, 2018), this paper will not introduce the trapezoidal/triangular shaping algorithm in detail.

The two shaping results are given in Fig. 4, which shows that the shaping results of the same negative exponential signal is truncated in the attenuation part and is repaired by the seventh-order successive approximation method. Comparison of the two shaping results shows that the shaping results of the distorted pulses have a lower amplitude and a narrower pulse width than the original pulse, as shown by the green lines of Fig. 4; on the other hand, the shaping results of the repaired pulses have the same amplitude and pulse width as the original pulse, as shown by the red lines of Fig. 4. In addition, compared with the formula based on equation (9), the

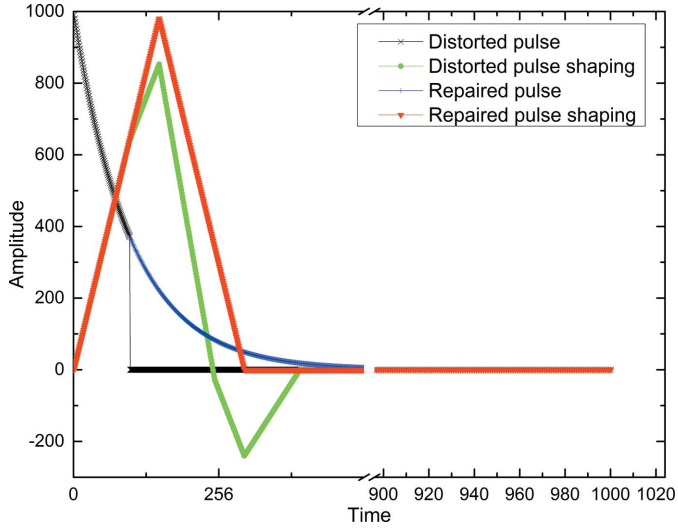

Figure 4
Triangular shaping results of the distorted negative exponential signal and repaired negative exponential signal. The black line is the distorted negative exponential signal. The red line is the triangular shaping result of the distorted negative exponential signal. The blue line is the repaired negative exponential signal. The red line is the triangular shaping result of the repaired negative exponential signal.

seventh-order successive approximation method is easier to implement in the FPGA and has a higher execution efficiency. In actual measurements, we will also use the seventh-order successive approximation method to repair the distorted pulses, and a comparison of the measured results will be introduced in the following section.

4. Experimental tests

In terms of actual measurement, the repairing of distorted pulses is realized in the FPGA. The key to the algorithm is the determination of the repairing conditions. The repairing condition used in this paper is different from the eliminating condition used for removing false peaks (Tang *et al.*, 2018). Considering that all the sampling points in the distorted pulse part turn to zero instantaneously, the zero point method is used to locate the sampling points that need to be repaired. In all pulse sequences, if the sampling points are equal to zero, they will need to be repaired by the seventh-order successive approximation method. If the next point is still zero, it will continue to iterate until a non-zero sampling point appears, and then the repaired negative exponential pulse sequence is shaped in the FPGA.

4.1. Experimental conditions

In order to verify the feasibility of this method, a ^{238}Pu source with activity of 10 mCi and one kind of copper ore sample are used as the measurement object on the basis of the simulation results mentioned above. In the measurement process, the pulse time constant is set to 3.2 µs, with an ADC sampling frequency of 20 MHz, a sampling period of 50 ns and a measurement time of 120 s. For the configuration of the experimental platform, we use a fast silicon drift detector (fast SDD) as the detector, with a collimated active area of 25 mm^2, detector thickness of 500 µm and Be window thickness of 0.5 mil.

Fig. 5 depicts a pulse sequence diagram captured arbitrarily during the actual measurement. In order to facilitate the observation of the experimental results, we only intercepted the pulse of a partial channel for analysis and comparison. Fig. 5 shows two overlapping peaks and one single peak; a pulse distortion occurred at the second descending edge of the second overlapped peaks, as shown by the red lines of the magnified region, in which the sampling point of the pulse jumps directly from 250 to 0. According to the repairing conditions mentioned above, once these zero sampling points are located, pulse repairing starts, and the repaired pulse is shown by the black line in Fig. 5, which not only restores all the sampling points but also restores the decay trend of the distorted pulse to roughly the same as that of the original pulse.

The reconstructed pulse sequence is shaped, and the corresponding spectrum is finally obtained through processing of the end circuit. Through the accurate analysis of the peak area of each peak in the spectrum, we can complete the

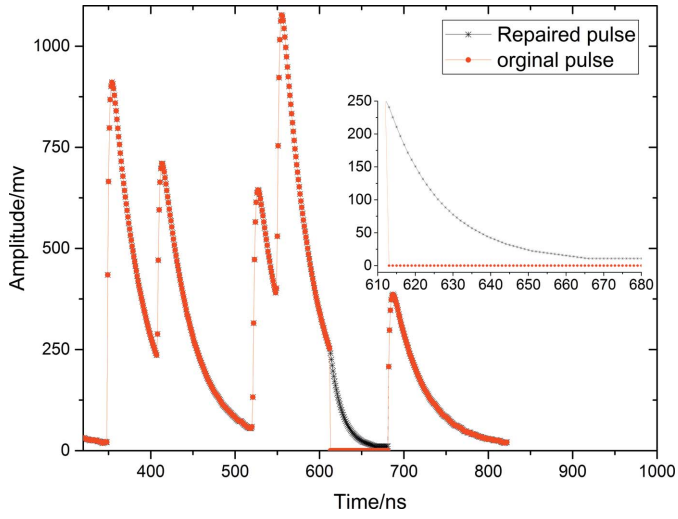

Figure 5
Actual measurement pulses of the ^{238}Pu standard source. The red line is an original pulse sequence which contains a distorted pulse, and the black line is the repaired pulse sequence.

quantitative analysis of the pulse repairing method, and have an intuitionistic quantification on the effect of the repairing.

In the previous research (Tang *et al.*, 2018), we drew the conclusion that the elimination of distorted pulses can remove false peaks in the whole spectrum. The purpose of this experiment is to prove that the method of pulse repairing can improve the counting rate on the basis of the pulse elimination method. Besides, this experiment also verifies that the counting value of the full spectrum obtained by the pulse repairing method is more stable than the pulse elimination method, and the statistical fluctuation is also reduced on the basis of more realistic counting.

4.2. Comparison of the repair effect

As mentioned above, equation (9) has the best repair effect. The decay speed of the seventh-order successive approximation method is faster than the original curve, but is very close to the original curve. In order to quantify the repairing effect of the two methods, equation (9) and the seventh-order successive approximation are used to obtain two spectra which will be compared with the original spectrum, whose distorted pulses will not be processed, as shown in Fig. 6.

The decay speed of the seventh-order successive approximation method is not completely consistent with the decay speed of the original pulse, resulting in the difference in amplitude between the repaired pulse shaping and the complete pulse shaping. As a result, the bottom width of the characteristic peak is broadened, but the elimination effect of the false peak, shown in Fig. 6, is not affected. Equation (9) almost completely fits the decay speed of the original pulse, so the false peaks are effectively eliminated and the bottom width of the characteristic peak is not affected.

The time constant of the original pulse, τ, is known in the MATLAB simulation, and the repair formula equation (9) is easy to implement by simulation. However, in a practical

Table 1
Comparison of peak area obtained by the pulse repairing and pulse elimination method.

Measurement	Method	S1	S2	S3	S4	S5	S6	S7	S8
First	Pulse elimination	9827	18896	29689	21031	126611	2159614	2516741	440965
	Pulse repairing	9973	19041	30115	21468	128849	2206349	2589151	458092
Second	Pulse elimination	9984	18946	29841	21000	126509	2160069	2516139	441183
	Pulse repairing	9982	19314	30088	21255	128817	2207343	2586949	456938
Third	Pulse elimination	10123	18852	29651	21105	126967	2158685	2517574	441606
	Pulse repairing	10172	19255	30040	21315	129115	2207270	2588156	458453
Fourth	Pulse elimination	9819	18981	29535	20990	126699	2161929	2517703	441317
	Pulse repairing	10094	19348	29952	21125	128591	2207913	2588549	456984
Fifth	Pulse elimination	9986	19127	29696	20901	126232	2162332	2517893	440628
	Pulse repairing	10077	19193	30089	21196	128877	2209996	2587063	457543
Sixth	Pulse elimination	9871	19151	29945	20868	126236	2161386	2516611	440505
	Pulse repairing	9981	19451	29955	21497	129342	2206414	2587909	456126
Seventh	Pulse elimination	10089	19044	29764	21052	126650	2161278	2517542	442239
	Pulse repairing	10158	19259	29761	21304	128448	2208808	2588904	457908
Eighth	Pulse elimination	9760	18958	29708	20923	126928	2162538	2517095	439693
	Pulse repairing	9856	19515	30230	21179	129251	2207610	2586926	458077
Ninth	Pulse elimination	10010	19151	29627	21154	126887	2159733	2515590	441842
	Pulse repairing	10071	19439	30258	21168	128798	2208648	2586922	457829
Tenth	Pulse elimination	9944	19101	29366	21587	126539	2159653	2513695	442358
	Pulse repairing	9949	19356	30478	21890	128849	2209533	2589412	457632
Average	Pulse elimination	9941	19020	29682	21061	126625	2160721	2516658	441233
	Pulse repairing	10031	19317	30096	21291	128893	2207988	2587994	457558

application the τ value of any negative exponential pulse is uncertain. In order to achieve an effective repair, the τ value of each pulse must be calculated, which is very time-consuming and increases computational load of the FPGA. However, the seventh-order successive approximation method only includes addition and division realized by shift arithmetic right (SAR), which has high efficiency. Therefore, this paper adopts the seventh-order successive approximation method as the best method for pulse repairing.

4.3. Peak area

In the experiment, the ^{238}Pu source was measured ten times using the pulse repairing and pulse elimination method. We chose any eight peaks for comparison in the measured spectrum. The peak area of the eight peaks was recorded as S1–S8, as shown in Table 1 and Fig. 7. The size of the peak area is different in the eight selected peaks, but the comparison results of the ten measurements show that the pulse repairing method improves the peak area of each peak, and it has a more obvious effect on the peak at high counting rates.

Fig. 7 shows the comparison result between the measured spectrum after the elimination of the distorted pulses and the spectrum obtained by repairing distorted pulses. If the FPGA does not repair the distorted pulses but eliminates them directly, the measurement result is the black line in Fig. 7. The red line is the measurement result of the pulse repairing method. Although both pulse repairing and pulse elimination methods can eliminate the false peaks, we find that the pulse elimination method will cause a loss of the counting rate. Therefore, we repair the distorted negative exponential signal into a complete negative exponential signal, which not only removes the false peak but also does not cause the loss of the counting rate. Thus the peak area is larger and more accurate.

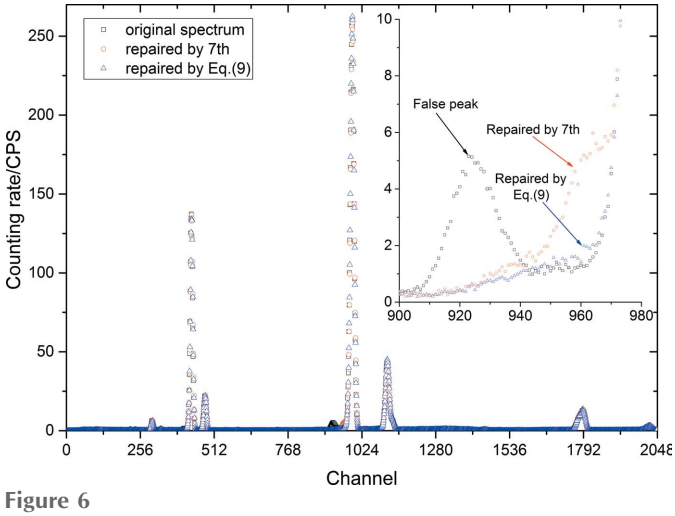

Figure 6
Comparison of different repair methods.

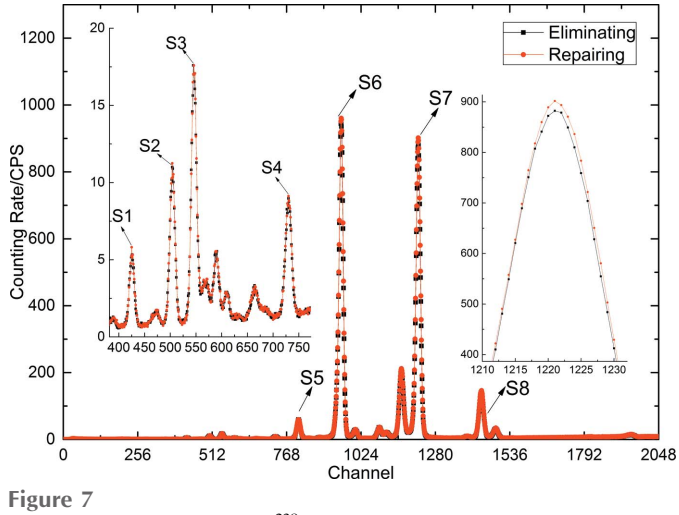

Figure 7
Comparison spectrum of the ^{238}Pu standard source obtained by the pulse elimination and pulse repairing method.

Table 2
Comparison of the count value obtained by the pulse repairing and pulse elimination methods.

$C_r = C_{repair}$; $C_e = C_{eliminate}$.

	C_r	C_e	$(C_r - C_e)/C_e$	C_r	C_e	$(C_r - C_e)/C_e$	C_r	C_e	$(C_r - C_e)/C_e$
Channel	1–2048	1–2048	–	1–768	1–768	–	768–1536	768–1536	–
1st measurement	6324465	6136640	3.06%	170238	154250	10.36%	5716682	5565590	2.71%
2nd measurement	6325511	6135383	3.10%	170487	154884	10.07%	5718501	5564030	2.78%
3rd measurement	6323431	6137275	3.03%	170385	154651	10.17%	5715407	5565375	2.70%
4th measurement	6321728	6138864	2.98%	169668	154372	9.91%	5715445	5567951	2.65%
5th measurement	6324494	6139515	3.01%	169736	155269	9.32%	5717628	5567322	2.70%
6th measurement	6319873	6137754	2.97%	170424	154726	10.15%	5713291	5565194	2.66%
7th measurement	6323491	6139968	2.99%	170381	154629	10.19%	5716978	5568698	2.66%
8th measurement	6323189	6138141	3.01%	169833	154810	9.70%	5715961	5566395	2.69%
9th measurement	6321793	6135764	3.03%	170179	155014	9.78%	5716800	5563850	2.75%
10th measurement	6321144	6133265	3.06%	170260	153773	10.72%	5713917	5562817	2.72%
Average value	6322911	6137257	–	170159	154637	–	5716061	5565722	–
Standard deviation	1743.75	2057.96	–	302.08	422.58	–	1607.92	1887.41	–

On the basis of Table 1, we compare ten groups of peak areas of any eight peaks selected in two ways: by the pulse elimination method and by the pulse repairing method. The count increase rate is defined as follows,

$$\text{Increase rate of peak area} = \big[(\text{peak area obtained by pulse repairing method}) - (\text{peak area obtained by pulse elimination method})\big] \big/ (\text{peak area obtained by pulse elimination method}). \quad (14)$$

Formula (14) is used to calculate the rates of increase of the peak areas, which are shown in Fig. 8. This figure includes nine lines of different colour, with each line having ten measurement points which were obtained by formula (14). Fig. 8 shows nine lines, eight of which represent the rate of increase of each peak area, respectively, and the red line represent the rate of increase of the total peak area of the eight peaks. It is easy to see that the count increase rate of the first to the fourth weak peaks fluctuates considerably, but the increase rate of each peak after S5 tends to be stable, and also that the sum of the peak areas of all peaks is relatively stable after the repairing, which is shown by the red line in Fig. 8.

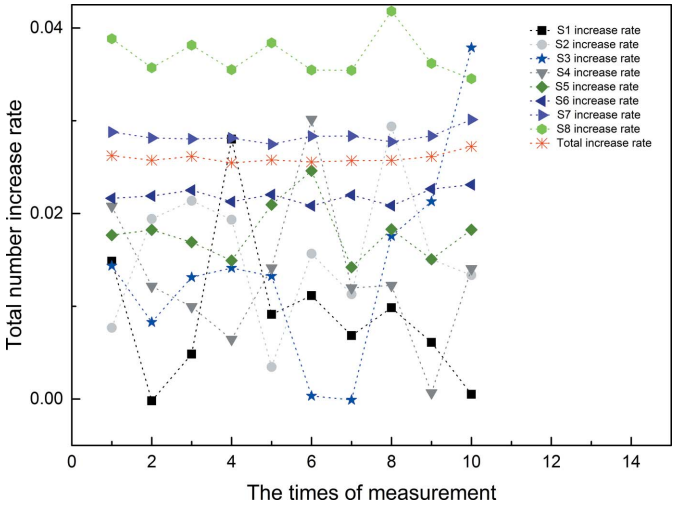

Figure 8
Increase rate of the peak area.

4.4. Counting-loss correction

Ten groups of measured data were obtained by using the pulse elimination method and the pulse repairing method, respectively. The total spectrum includes 2048 channels. As shown in Table 2, in this paper we have analyzed the count values of three channel ranges. The first range is the full spectrum, 2048 channels; the second range is the first 768 channels, which contain the S1–S4 four weak peaks mentioned in the previous article; and the third range is from channel 768 to channel 1536, which contains the four peaks S5–S8. A good measurement result requires not only that the counting value should be as large as possible, on the basis of ensuring that the counting value is true, but also that the statistical fluctuation should be reduced.

In Table 2, C represents the count value, A represents the average counting value of the ten measurement results, and S represents the standard deviation of the ten counting values. The average counting value obtained by the different processing methods can realize the quantization of increasing the proportion of the counting value, and the quantization result is shown in equation (15),

$$\text{Increase proportion of } C_{repair} = \frac{A_{repair} - A_{eliminate}}{A_{eliminate}}. \quad (15)$$

The average value of the ten measurement results of the full spectrum obtained after repairing is 6322911, and the average value when the pulse elimination method is used is 6137257; this gives an increase ratio for the counting value of 3% using equation (15), which is easily obtained by the pulse repairing method.

The statistical fluctuation of the ten measurement results obtained by each method is quantified by the standard deviation. It is easy to see that the standard deviation obtained by the pulse repairing method is always less than that obtained by the pulse elimination method in all channel ranges, which contain the full spectrum, the weak peak region and the strong peak area. That is to say, this experiment can verify that the

measurement results obtained by the pulse repairing method are more stable and the statistical fluctuation is smaller.

5. Conclusions

This paper presents a new method that not only solves the problem of false peaks located in front of the total energy peak but also increases the counting rate, when a fast SDD adopts a reset type preamplifier and pulse distortion occurs frequently. This method consists of three parts: theoretical deduction, method verification and experiment. The theoretical deduction part concludes that equation (9) and the seventh-order successive approximation method can be the theoretical basis of pulse repairing. The simulation verification part uses MATLAB as a tool for trapezoidal/triangular shaping, whose objects are a complete negative exponential pulse and a repaired negative exponential pulse. Comparison results show that the shaping result of a complete negative exponential pulse is indeed consistent with the shaping result of a repaired negative exponential pulse, and therefore we can conclude that both the equation (9) and the seventh-order successive approximation methods can repair distorted pulses effectively. Considering that the seventh-order successive approximation method is easier to implement, the actual measurement uses this method to repair distorted pulses. For the experiment, we chose a ^{238}Pu standard source as the measuring object to verify the repairing method mentioned above. According to the results of the measurement, the following conclusions can be drawn:

(i) The peak area of each peak in the spectrum obtained after pulse repairing has increased.

(ii) The peak area increase ratio for the strong peak is more stable than that of the weak peak.

(iii) For the same source, the sum of the peak area obtained by the pulse repairing method is increased by about 2.7% compared with the pulse elimination method.

(iv) The pulse repairing method can realize the correction of counting-loss, the increase ratio for the counting value obtained by the pulse repairing method is about 3%, and the statistical fluctuation of the counting value obtained by the pulse repairing method is lower than that obtained by the pulse elimination method.

Acknowledgements

This study was financially supported by the National Science and Technology Major Project Multidimensional high precision imaging logging series (2017ZX05019001). The authors thank Sichuan XSTAR Technology of M&C Co. Ltd, which provided the experimental platform.

References

Jakobson, C. G., Lavie D. & Nemirovsky, Y. (1995). *Proceedings of the 18th Convention of Electrical and Electronics Engineers in Israel*, 7–8 March 1995, Tel-Aviv, Israel. 5.5.4/1–5.5.4/5.

Jakobson, C. G. & Nemirovsky, Y. (1997). *IEEE Trans. Nucl. Sci.* **44**, 20–25.

Jordanov, V. T. (1994). *Nucl. Instrum. Methods Phys. Res. A*, **351**, 592–594.

Jordanov, V. T. (2003). *Nucl. Instrum. Methods Phys. Res. A*, **505**, 347–351.

Jordanov, V. T. & Knoll, G. F. (1994*b*). *Nucl. Instrum. Methods Phys. Res. A*, **345**, 337–345.

Jordanov, V. T., Knoll, G. F., Huber, A. C. & Pantazis, J. A. (1994*a*). *Nucl. Instrum. Methods Phys. Res. A*, **353**, 261–264.

Menaa, N., D'Agostino, P., Zakrzewski, B. & Jordanov, V. T. (2011). *Nucl. Instrum. Methods Phys. Res. A*, **652**, 512–515.

Morse, J. (2010). *Energy Resolving Semiconductor Detectors for X-ray Spectroscopy*, ESRF Lecture. European Synchrotron Radiation Facility, Grenoble, France.

Sun, H., Li, Y., Zhu, W., Wang, S. & Li, Y. (2005). *Nucl. Electron. Detect. Technol.* **25**, 77–80. (In Chinese.)

Tang, L., Yu, J., Zhou, J., Fang, F., Wan, W., Yao, J., Yu, S. & Liao, X. (2018). *Appl. Radiat. Isot.* **135**, 171–176.

Wang, M., Hong, X., Zhou, J. B., Liu, Y., Fei, P., Wan, W. J., Zhou, W., Ma, Y. J., Liu, Y. & Ding, W. C. (2018). *Appl. Radiat. Isot.* **137**, 280–284.

Zhen, J., Yang, Z. & Wang, L. (2002). *Nucl. Electron. Detect. Technol.* **22**, 152–154. (In Chinese.)

Zhou, J. *et al.* (2017). *Digital Analysis and Processing of Nuclear Signals*, 1st ed. Beijing: China Atomic Energy Publishing House. (In Chinese.)